On the correlation between fragility and stretching in glass-forming liquids

2007 J. Phys.: Condens. Matter 19 076102

(http://iopscience.iop.org/0953-8984/19/7/076102)

INSTITUTE OF PHYSICS PUBLISHING JOURNAL OF PHYSICS: CONDENSED MATTER

J. Phys.: Condens. Matter **19** (2007) 076102 (25pp) doi:10.1088/0953-8984/19/7/076102

On the correlation between fragility and stretching in glass-forming liquids

Kristine Niss[1], Cécile Dalle-Ferrier[1], Gilles Tarjus[2] and Christiane Alba-Simionesco[1]

[1] Laboratoire de Chimie Physique, CNRS-UMR 8000, Bâtiment 349, Université Paris-Sud, 91405 Orsay, France
[2] LPTMC, CNRS-UMR 7600, Université Pierre & Marie Curie, 4 Place Jussieu, 75252 Paris Cedex 05, France

Received 5 October 2006, in final form 14 December 2006
Published 15 January 2007
Online at stacks.iop.org/JPhysCM/19/076102

Abstract

We study the pressure and temperature dependences of the dielectric relaxation of two molecular glass-forming liquids, dibutyl phthalate and *m*-toluidine. We focus on two characteristics of the slowing down of relaxation, the fragility associated with the temperature dependence and the stretching characterizing the relaxation function. We combine our data with data from the literature to revisit the proposed correlation between these two quantities. We do this in light of constraints that we suggest to put on the search for empirical correlations among properties of glass-formers. In particular, we argue that a meaningful correlation is to be looked for between stretching and *isochoric* fragility, as both seem to be constant under isochronic conditions and thereby reflect the intrinsic effect of temperature.

(Some figures in this article are in colour only in the electronic version)

1. Introduction

With the goal of better understanding the physics of glasses and of glass formation, there has been a continuing search for empirical correlations among various aspects of the phenomenology of glass-formers. The most distinctive feature of glass formation being the rapid increase with decreasing temperature of the viscosity and relaxation times, correlations have essentially been looked for between the characteristics of the latter and other thermodynamic or dynamic quantities. Angell coined the term 'fragility' to describe the non-Arrhenius temperature dependence of the viscosity or (alpha) relaxation time and the associated change of slope on an Arrhenius plot [1]. He noticed the correlation between fragility and amplitude of the heat-capacity jump at the glass transition. Earlier, the Adam–Gibbs approach was a way to rationalize the correlation between the viscosity increase and the configurational or excess entropy decrease as one lowers the temperature [2]. Since then, a large number of

empirical correlations between 'fragility' and other properties of the liquid or of the glass have been found: for instance, larger fragility (i.e., stronger deviation from Arrhenius behaviour) has been associated with (i) a stronger deviation of the relaxation functions from an exponential dependence on time (a more important 'stretching') [3], (ii) a lower relative intensity of the boson peak [4], (iii) a larger mean square displacement at T_g [5], (iv) a smaller ratio of elastic to inelastic signal in the x-ray Brillouin-spectra [6], (v) a larger Poisson ratio [7] and (vi) a stronger temperature dependence of the elastic shear modulus, G_∞, in the viscous liquid [8].

Useful as they may be to put constraints on proposed models and theories of the glass transition, such correlations can also be misleading by suggesting causality relations where there are no such things. It seems therefore important to assess the robustness of empirically established correlations. In this respect, we would like to emphasize a number of points that are most often overlooked.

(1) Fragility involves a variation with temperature that *a priori* depends on the thermodynamic path chosen, namely constant pressure (isobaric) versus constant density (isochoric) conditions. On the other hand, many quantities that have been correlated to fragility only depend on the thermodynamic state at which they are considered: this is not the case for the variation of the excess entropy or of the shear modulus, or for the jump in heat capacity measured in differential scanning calorimetry, which are all path dependent, but the other properties are measured either at T_g, the glass-transition temperature, or in the glass, where they also relate to properties of the liquid as it falls out of equilibrium at T_g (there may be a residual path dependence due to the nonequilibrium nature of the glass, but it is quite different from that occurring in the liquid). *Which fragility then, isobaric or isochoric, should best be used in searching for correlations?*

(2) The quantities entering the proposed correlations are virtually always considered at T_g. This is the case for the commonly used measure of fragility, the 'steepness index', which is defined as the slope of the temperature dependence of the alpha-relaxation time on an Arrhenius plot with T scaled by T_g [9]. T_g is of course only operationally defined as the point at which the alpha-relaxation time (or the viscosity) reaches a given value, say 100 s for dielectric relaxation. The correlated properties are thus considered at a given relaxation time or viscosity. *What is the fate of the proposed correlations when one studies a different value of the relaxation time?*

(3) Almost invariably, comparisons involve properties measured at atmospheric pressure, for which the largest number of data are available. Since, as discussed in the preceding point, the properties are also considered at a given relaxation time, an obvious generalization consists in studying the validity of the reported correlations under 'isochronic' (i.e. constant relaxation time) conditions, by varying the control parameters such that the relaxation time stays constant. *How robust then are the correlations when one varies, say, the pressure along an isochrone?* In light of the above, our contention is that any putative correlation between fragility and another property should be tested, as far as possible, by varying the reference relaxation time, by varying the thermodynamic state along a given isochrone, and by changing the thermodynamic path along which variations, such as that defining the fragility, are measured.

A better solution would certainly be to correlate 'intrinsic' properties of glass-formers that do not depend on the chosen state point or relaxation time. A step toward defining such an 'intrinsic' fragility was made when it was realized that the temperature and the density dependences of the alpha-relaxation time and viscosity of a given liquid could be reduced to the dependence on a single scaling variable, $X = e(\rho)/T$, with $e(\rho)$ an effective activation energy characteristic of the high-temperature liquid [10, 11]. Evidence is merely empirical

and is supported by the work of several groups for a variety of glass-forming liquids and polymers [10–16]. The direct consequence of this finding is that the fragility of a liquid defined along an isochoric path is independent of density: the isochoric fragility is thus an intrinsic property, in contrast to the isobaric fragility. Although one could devise ways to characterize the isochoric fragility in a truly intrinsic manner, independently of the relaxation time, the common measure through the steepness index (see above) still depends on the chosen isochrone. In looking for meaningful correlations to this isochoric steepness index, it is clear however that one should discard quantities that vary with pressure (or equivalently with temperature) under isochronic conditions. As we further elaborate in this paper, the stretching parameter characterizing the shape of the relaxation function (or spectrum) is *a priori* a valid candidate, as there is some experimental evidence that it does not vary with pressure along isochrones [17].

The aim of the present work is to use the knowledge about pressure and temperature dependences of the liquid dynamics to test the robustness of proposed correlations between fragility and other properties. This is a continuation of the work presented in [18], where the focus was mainly on correlations between fragility of the liquid and properties of the associated glass. In this paper we specifically consider the correlation between fragility and stretching. The reported correlation between the two is indeed one of the bases of the common belief that both fragility and stretching are signatures of the cooperativity of the liquid dynamics.

We present new dielectric spectroscopy data on the pressure dependence of the alpha relaxation of two molecular glass-forming liquids. We focus on two systems which are well known in the field of the glass transition phenomenology: dibutyl phthalate (DBP) and *m*-toluidine; they are representative of a large set of molecular glass-forming liquids by their respective intermolecular interactions, and their dipole moments (2.4 and 1.43 D respectively) allow accurate dielectric measurements. DBP can be considered as a model van der Waals liquid, with the advantage of resisting crystallization under pressure, and *m*-toluidine possesses an additional feature related to its ability to form H-bonds and H-bonded induced clusters [19, 20].

We express the alpha-relaxation time as a function of the scaling variable $X = e(\rho)/T$ and evaluate the density dependence of $e(\rho)$ as well as the isochoric fragility. We also study the spectral shape and its pressure dependence along isochronic lines. We spend some time discussing the methodological aspects of the evaluation of the fragility and of the stretching from experimental data, as well as that of the conversion from P, T to P, ρ data. This provides an estimate of the error bars that one should consider when studying correlations. Finally, by combining our data with literature data we discuss the robustness of the correlation between fragility and stretching along the lines sketched above.

The paper is structured as follows. Section 2 introduces some concepts and earlier developments that are central for the discussion. In section 3 we present the experimental technique. Section 4 is devoted to the pressure, temperature, and density dependence of the relaxation time. In section 5 we analyse the spectral shape and its pressure and temperature dependence. Finally, in section 6 we combine the current results with literature data to assess the relation between fragility and stretching, stressing the need to disentangle temperature and density effects. Appendices A and B discuss some methodological points.

2. Background

2.1. Isochoric and isobaric fragilities

The fragility is a measure of how much the temperature dependence of the alpha-relaxation time (or alternatively the shear viscosity) deviates from an Arrhenius form as the liquid approaches

the glass transition. The most commonly used criterion is the so called steepness index,

$$m_{\mathrm{P}} = \left.\frac{\partial \log_{10}(\tau_\alpha)}{\partial T_{\mathrm{g}}/T}\right|_{\mathrm{P}} (T = T_{\mathrm{g}}), \tag{1}$$

where the derivative is evaluated at T_{g} and τ_α is expressed in seconds. Conventionally, the liquid is referred to as strong if m is small, that is 17–30, and fragile if m is large, meaning roughly above 60. In the original classification of fragility it was implicitly assumed that the relaxation time (or viscosity) was monitored at constant (atmospheric) pressure, as this is how the vast majority of experiments are performed. The conventional fragility is therefore the (atmospheric pressure) isobaric fragility, and, as indicated in equation (1), the associated steepness index is evaluated at constant pressure. However, the relaxation time can also be measured as a function of temperature along other isobars, and this will generally lead to a change in m_{P}. Moreover, it is possible to define an isochoric fragility and the associated index, m_ρ, obtained by taking the derivative at constant volume rather than at constant pressure. The two fragilities are straightforwardly related via the chain rule of differentiation,

$$m_{\mathrm{P}} = m_\rho + \left.\frac{\partial \log_{10}(\tau_\alpha)}{\partial \rho}\right|_T \left.\frac{\partial \rho}{\partial\, T_{\mathrm{g}}/T}\right|_{\mathrm{P}} (T = T_{\mathrm{g}}),$$

when both are evaluated at the same point $(T_{\mathrm{g}}(P), \rho(P, T_{\mathrm{g}}(P)))$. The isochoric fragility, m_ρ, describes the intrinsic effect of temperature, while the second term on the right-hand side incorporates the effect due to the change of density driven by temperature under isobaric conditions. It can be shown that the above relation can be rewritten as

$$m_{\mathrm{P}} = m_\rho(1 - \alpha_{\mathrm{P}}/\alpha_\tau) \tag{2}$$

where the unconventional α_τ is the isochronic expansivity [21], i.e., the expansivity along a line of constant alpha-relaxation time τ_α (the T_{g} line being a specific isochrone). The above result is purely formal and contains no assumptions. The implication of the result is that m_{P} is larger than m_ρ if $\alpha_{\mathrm{P}} > 0$ and $\alpha_\tau < 0$. It is well known that $\alpha_{\mathrm{P}} > 0$ in general. The fact that α_τ is negative arises from the empirical result that the liquid volume always decreases when heating while following an isochrone.

Within the last decade a substantial number of relaxation-time and viscosity data have been collected at different temperatures and pressures/densities. On the basis of the existing data, it is reasonably well established that the temperature and density dependences of the alpha-relaxation time can be expressed in a scaling form as [10–16].

$$\tau_\alpha(\rho, T) = F\left(\frac{e(\rho)}{T}\right). \tag{3}$$

It is seen directly from equation (3) that $X(\rho, T) = e(\rho)/T$, when evaluated at T_{g}, has the same value at all densities ($X_{\mathrm{g}} = e(\rho)/T_{\mathrm{g}}(\rho)$) if $T_{\mathrm{g}}(\rho)$ is defined as the temperature where the relaxation time has a given value (e.g., $\tau_\alpha = 100$ s). Exploiting this fact, it is easy to show [11, 22] that the scaling law implies that the isochoric fragility is independent of density. For instance, the isochoric steepness index, when evaluated at a T_{g} corresponding to a fixed relaxation time, is given by

$$m_\rho = \left.\frac{\mathrm{d}\log_{10}(\tau_\alpha)}{\mathrm{d}T_{\mathrm{g}}/T}\right|_\rho (T = T_{\mathrm{g}}) = F'(X_{\mathrm{g}})\frac{\mathrm{d}X}{\mathrm{d}T_{\mathrm{g}}/T}(T = T_{\mathrm{g}}) = X_{\mathrm{g}}F'(X_{\mathrm{g}}). \tag{4}$$

The fact that the relaxation time τ_α is constant when X is constant means that the isochronic expansion coefficient α_τ is equal to the expansion coefficient at constant X. Using this and the general result $(\frac{\partial \rho}{\partial T})_X(\frac{\partial X}{\partial \rho})_T(\frac{\partial T}{\partial X})_\rho = -1$, it follows that

$$\frac{1}{\alpha_\tau} = -T_{\mathrm{g}}\frac{\mathrm{d}\log e(\rho)}{\mathrm{d}\log \rho}, \tag{5}$$

which inserted in equation (2) leads to

$$m_{\mathrm{P}} = m_\rho \left(1 + \alpha_{\mathrm{P}} T_{\mathrm{g}} \frac{\mathrm{d}\log e(\rho)}{\mathrm{d}\log \rho}\right), \tag{6}$$

where m_{P}, m_ρ and α_{P} are evaluated at T_{g}.

When liquids have different isobaric fragilities, it can be thought of as due to two reasons: a difference in the intrinsic isochoric fragility, m_ρ, or a difference in the relative effect of density, characterized by $\alpha_{\mathrm{P}} T_{\mathrm{g}}$ and the parameter $x = \frac{\mathrm{d}\log e(\rho)}{\mathrm{d}\log \rho}$. We analyse the data in this frame.

2.2. *Relaxation-time dependent fragility*

The following considerations hold for isochoric and isobaric conditions alike. The ρ or P subscript is therefore omitted in this section.

The fragility is usually characterized by a criterion evaluated at T_{g}, i.e. the temperature at which the relaxation time reaches $\tau_\alpha = 100$–1000 s. The same criterion, e.g. the steepness index, can however equally well be evaluated at a temperature corresponding to another relaxation time, and this is also found more often in the literature, mainly to avoid the extrapolation to long times. So defined, the 'fragility' for a given system can be considered as a quantity which is dependent on the relaxation time at which it is evaluated:

$$m(\tau) = \frac{\mathrm{d}\log_{10}(\tau_\alpha)}{\mathrm{d}T_\tau/T}(T = T_\tau) \tag{7}$$

where $\tau_\alpha(T_\tau) = \tau$ defines the temperature T_τ. (T_{g} is a special case with $\tau \approx 100$–1000 s.)

An (extreme) strong system is a system for which the relaxation time has an Arrhenius behaviour,

$$\tau_\alpha(T) = \tau_\infty \exp\left(\frac{E_\infty}{T}\right), \tag{8}$$

where E_∞ is a temperature and density independent activation energy (measured in units of temperature). Inserting this in the expression for the relaxation-time dependent steepness index (equation (7)) gives

$$m_{\mathrm{strong}}(\tau) = \log_{10}(\tau/\tau_\infty) \tag{9}$$

which gives the value $m_{\mathrm{strong}}(\tau = 100\ \mathrm{s}) = 15$ (assuming $\log_{10}(\tau_\infty/\mathrm{s}) = -13$) and decreases to $m_{\mathrm{strong}}(\tau = \tau_\infty) = 0$ as the relaxation time is decreased. This means that even for a strong system the steepness index is relaxation-time dependent. In order to get a proper measure of departure from Arrhenius behaviour it could therefore be more adequate to use the steepness index normalized by that of a strong system:

$$m_n(\tau) = \frac{m(\tau)}{m_{\mathrm{strong}}(\tau)} = \frac{\frac{\mathrm{d}\log_{10}(\tau_\alpha)}{\mathrm{d}T_\tau/T}}{\log_{10}(\tau/\tau_\infty)}. \tag{10}$$

$m_n(\tau)$ will take the value 1 at all relaxation times in a system where the relaxation time has an Arrhenius behaviour. Such a normalized measure of fragility has been suggested before [23–25]. For instance, Olsen and co-workers [25] have introduced the index

$$I = -\frac{\mathrm{d}\log E(T)}{\mathrm{d}\log T} \tag{11}$$

where $E(T)$ is a temperature dependent activation energy defined by $E(T) = T\ln(\tau_\alpha/\tau_\infty)$. The relation between the steepness index and the Olsen index is [25]

$$I(\tau) = \frac{m(\tau)}{\log_{10}\left(\frac{\tau}{\tau_\infty}\right)} - 1 = m_n(\tau) - 1. \tag{12}$$

$I(\tau)$ takes the value of zero for strong systems at all relaxation times. Typical glass forming liquids display an approximate Arrhenius behaviour at high temperatures and short relaxation times; in this limit $I(\tau) = 0$ and it increases as the temperature dependence starts departing from the Arrhenius behaviour. Typical values of I at $T_g(\tau = 100$ s) range from $I = 3$ to 8, corresponding to steepness indices of $m = 47$–127.

Finally, we note in passing that relaxation-time independent measures of fragility can be formulated through fitting formulae: this is the case for instance of the fragility parameter D in the Vogel–Tammann–Fulcher (VTF) formula or of the frustration parameter B in the frustration-limited domain theory [26].

3. Experiments

The dielectric cell is composed of two gold-coated electrodes separated by small Teflon spacers. The distance between the spacers is 0.3 mm and the area is 5.44 cm^2, giving an empty capacitance of 16 pF. The electrodes are totally immersed in the liquid sample, which is sealed from the outside by a Teflon cell. The electric contacts are pinched through the Teflon. The compression is performed using liquid pentane, which surrounds the Teflon cell from all sides. The Teflon cell has one end with a thickness of 0.5 mm in order to insure that the pressure is well transmitted from the pentane to the liquid sample. The pressure is measured by using a strain gauge. The cooling is performed by a flow of thermostatted cooling liquid running inside the autoclave. The temperature and the temperature stability are monitored by two PT100 sensors placed 2 and 0.3 cm from the sample. The temperature is held stable within $\pm 0.1\,^\circ$C for a given isotherm. The temperature during the time it takes to record a spectrum is stable within $\pm 0.01\,^\circ$C.

The set-up insures a hydrostatic pressure because the sample is compressed from all sides. It is moreover possible to take spectra both under compression and decompression. By doing so and returning to the same P–T conditions after several different thermodynamic paths we have verified that there was no hysteresis in the pressure dependence of the dynamics. This serves to confirm that the liquid is kept at thermodynamic equilibrium at all stages.

The capacitance was measured using an HP 4284A LCR meter, which covers the frequency range from 100 Hz to 1 MHz. The low-frequency range from 100 to 1 Hz was covered using an SR830 lock-in.

The samples, dibutyl phthalate (DBP) and *m*-toluidine, were acquired from Sigma-Aldrich. The *m*-toluidine was twice distilled before usage. The DBP was used as acquired.

Liquid *m*-toluidine was measured on one isotherm at 216.4 K. DBP was measured along four different isotherms, 205.5, 219.3, 236.3 and 253.9 K, at pressures up to 400 MPa. DBP was moreover measured at different temperatures along two isobars: atmospheric pressure and 230 MPa. The pressure was continuously adjusted in order to compensate for the decrease of pressure which follows from the contraction of the sample due to decreasing temperature. It is of course always possible to reconstruct isobars based on experiments performed under isotherm conditions. However, such a procedure mostly involves interpolation of the data, which is avoided by performing a strictly isobaric measurement. For DBP we have obtained relaxation-time data at times shorter than $10^{-6.5}$ s by using the high-frequency part of the spectrum and assuming time–temperature and time–pressure superposition (TTPS). Although TTPS is not followed to a high precision (see section 5.1), the discrepancies lead to no significant error on the determination of the relaxation time. This is verified by comparison to atmospheric-pressure data from the literature (see figure 1).

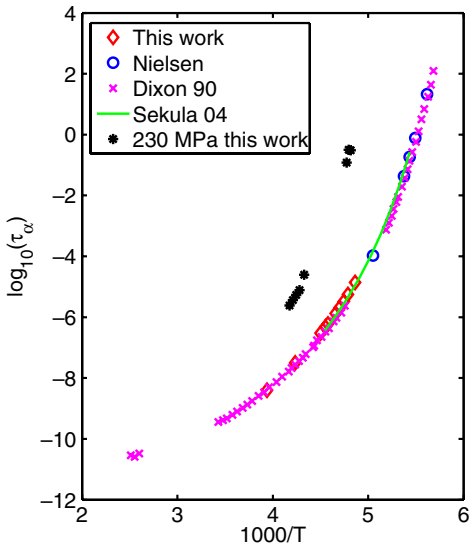

Figure 1. Temperature dependence of the alpha-relaxation time (from dielectric measurements, $\tau_\alpha = 1/\omega_{\text{peak}}$) of liquid DBP at atmospheric pressure and at 230 MPa (Arrhenius plot). Data at atmospheric pressure from other groups are also included: unpublished data from Nielsen [35], the VTF fit of [27] shown in the range where it can be considered as an interpolation of the original data, and data taken from figure 2(a) in [29].

4. Alpha-relaxation time and fragility

4.1. Dibutyl phthalate

The DBP data at atmospheric pressure are shown in figure 1 along with literature results. $T_g(P_{\text{atm}}) = 177$ K, when defined as the temperature at which $\tau_\alpha = 100$ s. We also present the data taken at $P = 230$ MPa in this figure. It is clearly seen that T_g increases with pressure. An extrapolation of the data to $\tau_\alpha = 100$ s gives $T_g = 200$ K for $P = 230$ MPa, corresponding to $dT_g/dP \approx 0.1$ K MPa^{-1}. This corresponds well to the pressure dependence of T_g (at $\tau_\alpha = 1$ s) reported by Sekula *et al* [27], based on measurements made at pressures higher than 600 MPa. The dependence is however stronger than that reported by Fujimori *et al* [28] based on isothermal calorimetry, for which $dT_g/dP = 0.06$ K MPa^{-1}. This indicates that the calorimetric and the dielectric relaxations may have somewhat different dependences on pressure.

In figure 2 we illustrate the determination of T_g and of the steepness index m_P for the atmospheric-pressure data, using the part of the data of figure 1 with a relaxation time longer than a millisecond. Along with the data we show the VTF fit from Sekula *et al* [27] extrapolated to low temperatures, which gives $T_g = 177.4$ K and $m_P = 84$. We have also performed a new VTF fit restricted to the data in the 10^{-6}–10^2 s region. The result of this fit yields $T_g = 176.6$ K and $m_P = 82$. Finally, we have made a simple linear estimate of $\log_{10} \tau_\alpha$ as a function of $1/T$ in the temperature range shown in the figure. This linear slope fits the data close to T_g better than any of the VTF fits. The corresponding glass transition temperature and steepness index are $T_g = 176$ K and $m_P = 70$. This illustrates that the determination of T_g is rather robust, while this is less so for the steepness index. This latter depends on how it is obtained, and the use of extrapolated VTF fits can lead to an overestimation. (Of course, a VTF fit made over a very narrow range, e.g. 10^{-2}–10^2 s, will agree with the linear fit, because it becomes

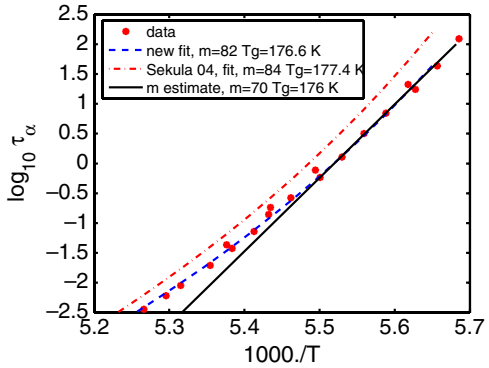

Figure 2. Atmospheric-pressure data of figure 1 with relaxation times longer than a millisecond (symbols). Also shown are the VTF fit from [27] extrapolated to low temperatures (dashed–dotted line), a new VTF fit made by using displayed data in the 10^{-6} s -10^{2} region (dashed line), and the estimated slope of the data in the long-time region (full line). The T_g values estimated from these three methods are very similar, whereas the fragility varies significantly from $m = 65$ to 85.

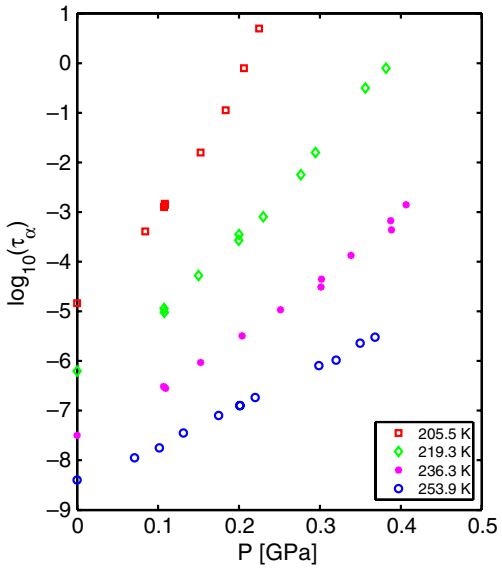

Figure 3. Alpha-relaxation time of DBP (from dielectric measurements, $\tau_\alpha = 1/\omega_{\text{peak}}$) as a function of pressure along four different isotherms (log–linear plot).

essentially linear over the restricted range.) The fragility of DBP has earlier been reported to be $m_P = 69$ [3], based on the data of Dixon *et al* [29]. We take $m_P = 75$ as a representative value.

The relaxation-time data along four different isotherms are displayed as a function of pressure in figure 3.

In order to separate the relative effects of density and temperature it is convenient to express the relaxation time as a function of density and temperature rather than pressure and temperature. To do this, we need the pressure and temperature dependences of the density. However, for liquid DBP such data is only available at high temperature [30].

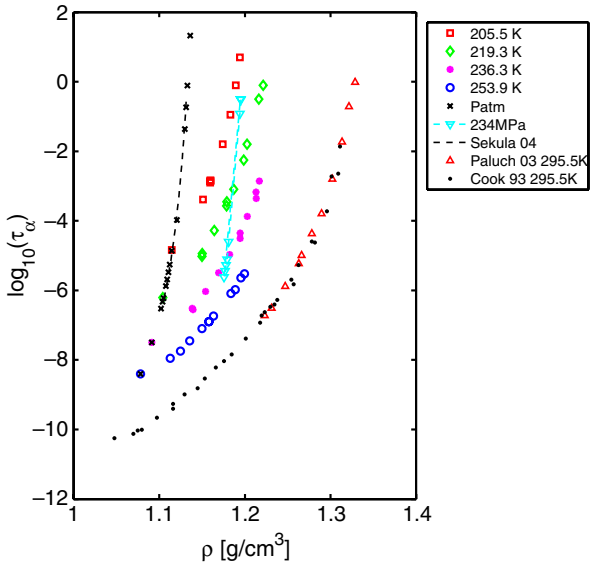

Figure 4. Logarithm of the alpha-relaxation time of DBP versus density (see the text regarding the calculation of density). Included are data from this work along with dielectric data of Paluch from figure 3 in [33], and viscosity data from Cook [31]. The viscosity data are shifted arbitrarily on the logarithmic scale in order to make the absolute values correspond to the dielectric data of [33], which are taken at the same temperature.

In order to extrapolate the equation of state to low temperature we have applied the following scheme. When calculated from the data in [30], the expansion coefficient α_P shows a weak decrease with decreasing temperature. We therefore assume that the temperature dependence of α_P is linear over the whole temperature range and integrate with respect to temperature to obtain the density along the atmospheric-pressure isobar. In the whole temperature range of [30], the pressure dependence of the density is well described by fits to the Tait equation with temperature-dependent adjustable parameters 'c' and 'b' [31] (which are directly related to the compressibility and its first-order pressure derivative). We have linearly extrapolated the temperature dependence of these parameters and used the Tait equation to calculate the pressure dependence along each isotherm. Extrapolating the derivatives rather than the density itself is expected to lead to smaller errors on the latter. In addition, we have checked that this procedure gives physically reasonable pressure and temperature dependences of the expansivity and of the compressibility [32].

Figure 4 shows the density dependence of the alpha-relaxation time along the four different isotherms, the atmospheric-pressure isobar and the 230 MPa isobar. We have also included the room-temperature dielectric data of Paluch *et al* [33]. For DBP the viscosity data and the dielectric relaxation time do not decouple under pressure [27], and we have therefore also included the room-temperature viscosity data of Cook *et al* [33].

In figure 5 we show the data of figure 4 plotted as a function of the scaling variable ρ^x/T, choosing for x the value that gives the best collapse for the data of this work. This corresponds to testing the scaling in equation (3) by assuming that $e(\rho)$ is a power law. The data taken at low density collapse quite well with $x = 2.5$, while this is not true for the data of Paluch [33] taken at densities higher than approximately 1.2 g cm^{-3}. It is possible to make all the data collapse by allowing $e(\rho)$ to have a stronger density dependence at higher densities. In figure 6

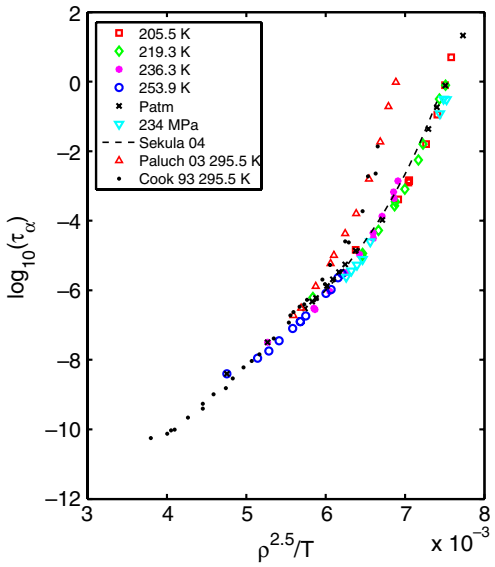

Figure 5. The alpha-relaxation times shown in figure 4 plotted as a function of $\rho^{2.5}/T$.

we show the data as a function of $e(\rho)/T$, where we have constructed the density dependence of $e(\rho)$ in order to get a good overlap of all the data (we did not look for the best collapse, but merely evaluated the change of the isochronic expansivity: see section 2). The resulting density dependence of $e(\rho)$ is shown in figure 6 along with the $\rho^{2.5}$ power law. Note that the quality of the data collapse depends only on the density dependence of $e(\rho)$, not on its absolute value. The constructed $e(\rho)$ has an apparent 'power-law' exponent $x(\rho) = \mathrm{d}\log e(\rho)/\mathrm{d}\log\rho$ that increases from 1.5 to 3.5 with density in the range considered. In any case, the absence of collapse in figure 5 cannot be explained by errors in estimating the PVT data: this is discussed in more detail in appendix A. In another recent paper [34] it is reported that DBP has a constant power-law exponent of 3.2. However, the PVT-data used in this paper do not agree at all with the data known in the literature (either absolute value or pressure and temperature dependences).

As a last note regarding the $e(\rho)/T$ scaling in figure 6, we want to stress that we cannot test the scaling (equation (3)) in the density range above 1.25 g cm^{-3}, where there is only one set of data. (This is why we did not attempt to fine tune $e(\rho)$ to find the best collapse; see above.) Indeed, with a unique set of data in a given range of density it is always possible to construct $e(\rho)$ in this range to make the data overlap with data taken in other density ranges.

We have determined the ratio between the isochoric fragility and the isobaric fragility at atmospheric pressure by calculating α_τ along the isochrone of 100 s and inserting it in equation (2). This leads to $m_\mathrm{P}/m_\rho \approx 1.2$. In figure 7 we show the isobaric data taken at atmospheric pressure and at 230 MPa scaled by their respective $T_\mathrm{g}(P)$. No significant pressure dependence of the isobaric fragility is observed when going from atmospheric pressure to 230 MPa, which is consistent with the result of reference [27]. The pressure independence of m_P is connected to the relatively low value of $m_\mathrm{P}/m_\rho = 1.2$ (typical values are 1.1–2 [11]); m_ρ is pressure independent and the ratio m_P/m_ρ cannot be lower than one (see equation (2)), so that m_P can at most decrease by 20% from its atmospheric-pressure value. Moreover, the increase in $\frac{\mathrm{d}\ln(e(\rho))}{\ln\rho}$ with density will tend to cancel the decrease in $\alpha_\mathrm{P}T_\mathrm{g}$, which is usually responsible for the decrease in fragility with increasing pressure.

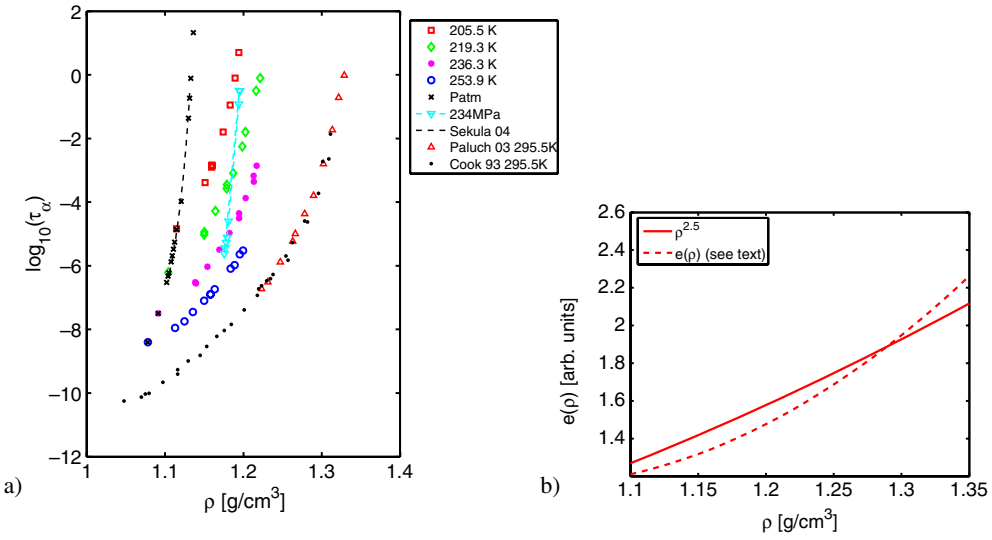

Figure 6. (a) The alpha-relaxation times shown in figure 4 plotted as a function of $X = e(\rho)/T$, with increasing $\mathrm{d}\log e(\rho)/\mathrm{d}\log\rho$ as ρ increases. (b) Density-dependent activation energy $e(\rho)$ (dashed line) used in the scaling variable $X = e(\rho)/T$ for collapsing data in (a) (the associated $x(\rho) = \mathrm{d}\log e(\rho)/\mathrm{d}\log\rho$ increases from 1.5 to 3.5 in the density range under study). We also display the power law giving the best scaling, $\rho^{2.5}$, at low density (full line).

4.2. m-toluidine

The glass transition temperature at atmospheric pressure is $T_g = 187$ K (for $\tau_\alpha = 100$ s) and the isobaric fragility based on dielectric spectra is reported to be $m_P = 82 \pm 3$ [36, 37]. (There has been some controversy about the dielectric relaxation in *m*-toluidine; see [36] and references therein.)

In the inset of figure 8 we show the pressure-dependent relaxation time at 216.4 K. Extrapolating the data to $\tau_\alpha = 100$ s leads to $P_g = 340 \pm 10$ MPa, corresponding to $\mathrm{d}T_g/\mathrm{d}P = 0.085$ K MPa^{-1}. This value is, as we also saw in the case of DBP, about a factor of two higher than the $\mathrm{d}T_g/\mathrm{d}P = 0.045$ K MPa^{-1} reported for the calorimetric glass transition by [38]. This could suggest that this type of decoupling is general; however, there are also examples where no such decoupling is found [39].

As for DBP, we wish to convert the temperature and pressure dependences of the relaxation time to the temperature and density dependences. Density data are available along four isotherms in the 278.4–305.4 K range for pressures up to 300 MPa [40]. Tait fits and thermal expansivity in this range were extrapolated by using the scheme described above for DBP in order to determine density both as a function of temperature down to T_g and as a function of pressure on the 216.4 K isotherm. In figure 8 we show the alpha-relaxation time as a function of density. The data taken at atmospheric pressure and the data taken along the 216.4 K isotherm cover two different ranges in density. It is therefore not possible from these data to verify the validity of the scaling in $X = e(\rho)/T$. We therefore assume that the scaling is possible. Moreover, due to the paucity of the data we describe $e(\rho)$ by a simple power law, $e(\rho) = \rho^x$. We find the exponent x by exploiting the fact that the scaling variable $X = e(\rho)/T$ is uniquely fixed by the value of the relaxation time; applying this at T_g, namely setting $X_g(P_{atm}) = X_g(216\ \mathrm{K})$, leads to $x = 2.3$ and gives a ratio of $m_P/m_\rho = 1.2$.

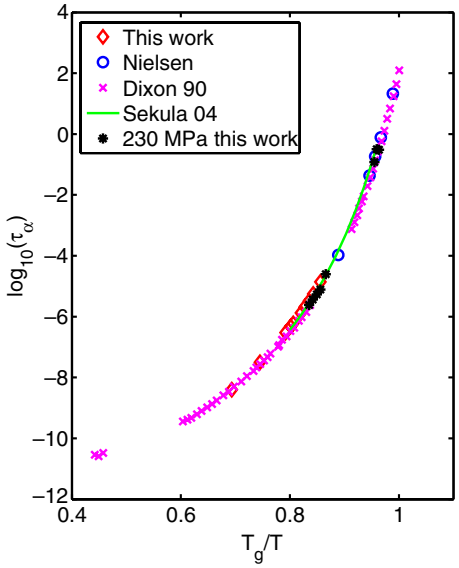

Figure 7. Arrhenius plot of the alpha-relaxation time of DBP at atmospheric pressure and at 230 MPa, when the temperature is scaled with the pressure dependent T_g, $T_g(P_{atm}) = 176$ K and $T_g(230\ \text{MPa}) = 200$ K. As in figure 1, data from other groups are also included: unpublished data from Nielsen [35], the VTF fit of [27], shown in the range where it can be considered as an interpolation of the original data, and data taken from figure 2(a) in [29].

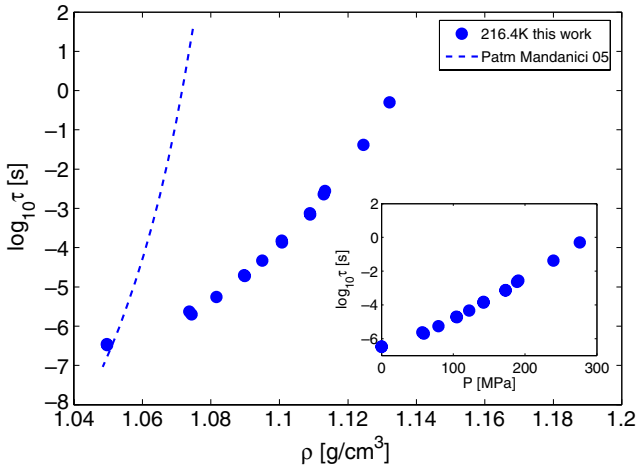

Figure 8. Logarithm of the alpha-relaxation time of *m*-toluidine as a function of density along the isotherm $T = 216.4$ K (symbols). The VTF fit of the atmospheric-pressure data of Mandanici *et al* [36] is also shown in the range where the fit can be considered as an interpolation of the data (dashed line). The inset shows the alpha-relaxation time of *m*-toluidine as a function of pressure along the isotherm $T = 216.4$ K.

5. Spectral shape and stretching

The shape of the relaxation function (or spectrum), most specifically its distinctly nonexponential (or non-Debye) character in the viscous regime, is taken as one of the important

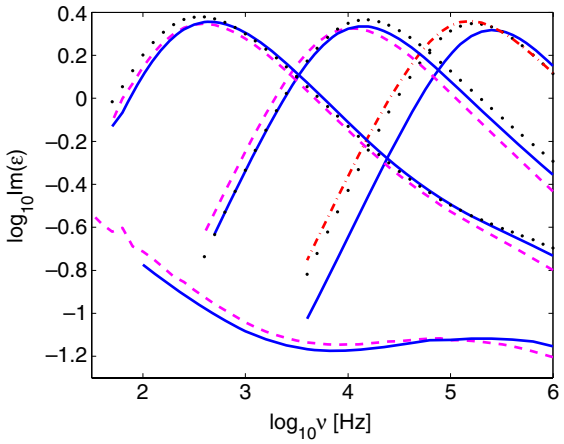

Figure 9. Log–log plot of the frequency-dependent dielectric loss of DBP. The curves can be sorted into four groups, each group having roughly the same peak frequency: (i) dashed–dotted (red) curve, $T = 253.9$ K, $P = 320$ MPa; black dots, $T = 236.3$ K, from right to left $P = 153$ MPa, $P = 251$ MPa, $P = 389$ MPa; full (blue) line, $T = 219.3$ K, from right to left $P = 0$ MPa, $P = 108$ MPa, $P = 200$ MPa, $P = 392$ MPa; dashed (magenta) curve, $T = 206$ K, from right to left $P = 0$ MPa, $P = 85$ MPa, $P = 206$ MPa.

features of glass-forming materials. Characterizing and quantifying this effect is however not fully straightforward and has led to diverging interpretations. First of all, the shape of the relaxation function or spectrum may change with the experimental probe considered. Even when restricting comparison to a single probe, here dielectric relaxation, there is no consensus on how to best characterize the shape. We discuss in appendix B various procedures that are commonly used and we test their validity on one representative spectrum. For reasons detailed in that appendix, we focus in the following on the Cole–Davidson fitting form.

5.1. Dibutyl phthalate

The frequency-dependent dielectric loss for a selected set of different pressures and temperatures is shown in figure 9. The first observation is that cooling and compressing have a similar effect as both slow down the alpha relaxation and separate the alpha relaxation from higher-frequency beta processes. The data displayed are chosen so that different combinations of temperature and pressure give almost the same relaxation times. However, the correspondence is not perfect. In figure 10 we have thus slightly shifted the data, by at most 0.2 decade, in order to make the peak positions overlap precisely. This allows us to compare the spectral shapes directly. It can be seen from the figure that the shape of the alpha peak itself is independent of pressure and temperature for a given value of the alpha-relaxation time (i.e. of the frequency of the peak maximum), while this is not true for the high-frequency part of the spectra, which is strongly influenced by the beta-relaxation peak (or high-frequency wing). When comparing datasets that have the same alpha-relaxation time, one finds that the high-frequency intensity is higher for the pressure–temperature combination corresponding to high pressure and high temperature.

In figure 11 we show all the datasets of figure 9 superimposed and we zoom in on the region of the peak maximum. The overall shape of the alpha relaxation is very similar at all pressures and temperatures. However, looking at the data in more detail, one finds a significantly larger degree of collapse between spectra which have the same relaxation time, whereas a small

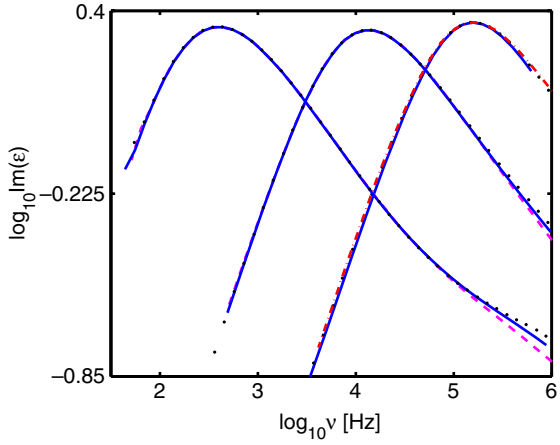

Figure 10. Same dielectric loss data of DBP as in figure 9 with a slight shift of the peak frequencies (less than 0.2 decade) to make the data taken under quasi-isochronic conditions precisely coincide. The symbols are the same as in figure 9, but the data at $T = 206$ K and $P = 206$ MPa and $T = 219.3$ K and $P = 392$ MPa are not shown.

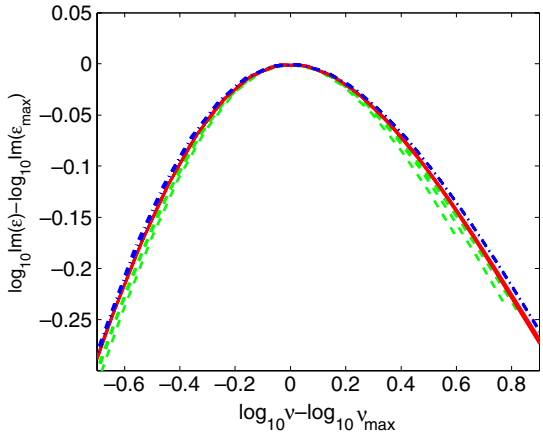

Figure 11. The same dielectric-loss data as in figures 9 and 10, with the frequency and intensity now scaled by the values at the maximum. We show only 1.5 decades in frequency in order to magnify the details. Notice a small broadening as the characteristic relaxation time increases. Dashed–dotted (blue) lines are three different data sets with $\log_{10} \nu_{\max} \approx 2.6$ ($P = 320$ MPa, $T = 253.9$ K; $P = 153$ MPa, $T = 236.3$ K, and $P = 0$ MPa, $T = 219.3$ K). Full (red) lines are three data sets with $\log_{10} \nu_{\max} \approx 4.1$ ($P = 251$ MPa, $T = 236.3$ K; $P = 108$ MPa, $T = 219.3$ K, and $P = 0$ MPa, $T = 205.6$ K). Dashed (green) lines are three data sets with $\log_{10} \nu_{\max} \approx 5.2$ ($P = 339$ MPa, $T = 236.3$ K; $P = 200$ MPa, $T = 219.3$ K, and $P = 85$ MPa, $T = 205.6$ K).

broadening of the alpha peak is visible as the relaxation time is increased. At long relaxation times there is a perfect overlap of the alpha-relaxation peaks which have the same relaxation time. At shorter relaxation time, $\log_{10}(\omega_{\max}) \approx 5$, the collapse is not as good: the peak gets slightly broader when pressure and temperature are increased along the isochrone. In all cases, the alpha peak is well described by a Cole–Davidson (CD) shape. The β_{CD} goes from 0.49 to 0.45 on the isochrone with the shortest relaxation time and decreases to about 0.44 close to T_{g} at all pressures. On the other hand, a Kohlrausch–William–Watts (KWW) fit close to T_{g} gives

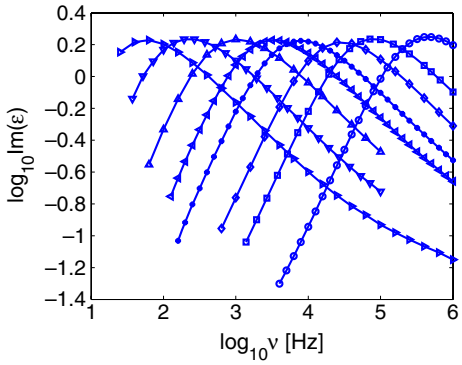

Figure 12. Log–log plot of the frequency-dependent dielectric loss of *m*-toluidine at $T = 216.4$ K and pressures 0, 59, 79, 105, 122, 142, 173 and 191 MPa. The peak shifts left as pressure is applied. Lines are guides to the eye.

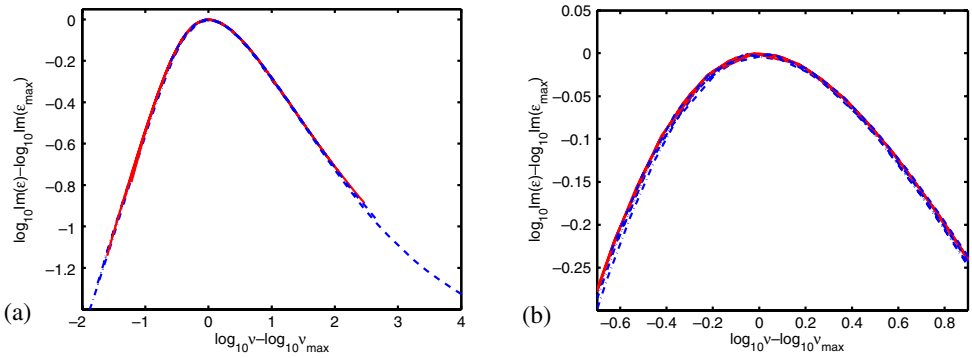

Figure 13. Same dielectric-loss data as in figure 12, now with the intensity and the frequency scaled by the values of the peak maximum. (b) A zooming in of the data in (a) to focus on the alpha-relaxation region near the peak maximum.

$\beta_{\mathrm{KWW}} = 0.65$. A detailed discussion of the fitting procedures and of the relation between CD and KWW descriptions is given in appendix B.

5.2. m-toluidine

The frequency-dependent dielectric loss of *m*-toluidine for several pressures along the $T = 216.4$ K isotherm is shown in figure 12. The data are then superimposed by scaling the intensity and the frequency by the intensity and the frequency of the peak maximum, respectively: this is displayed in figure 13. When zooming in (figure 13(b)) we still see almost no variation of the peak shape. For the present set of data, pressure–time superposition is thus obeyed to a higher degree than in DBP, and the changes are too small to give any pressure dependence in the parameters when fitting the spectra. The Cole–Davidson fit to the *m*-toluidine gives $\beta_{\mathrm{CD}} = 0.42$ (see also appendix B). Mandanici [36] and co-workers have reported a temperature independent value of $\beta_{\mathrm{CD}} = 0.45$ for data taken at atmospheric pressure in the temperature range 190–215 K, a value that is compatible with ours. While the alpha-relaxation peak seems not to change in shape in the pressure range studied, it is seen that there is a change in slope at high frequencies at high pressure. This suggests that a beta process might appear if one goes to even higher pressures.

6. Discussion

6.1. Correlations with fragility

As discussed in the introduction, the temperature dependence of the alpha-relaxation time (or of the viscosity) is usually considered as the most important phenomenon to understand in glass science. Isobaric fragility is then often used to characterize the viscous slowing down and its measures, such as the steepness index, are then considered as fundamental parameters. Many studies have been aimed at investigating which other properties of the liquid and of the associated glass correlate to fragility. Such correlations have been empirically established by comparing rather large sets of systems covering a wide spectrum of fragilities.

In the literature, the finding of a correlation between fragility and some other property is always interpreted as indicating that the property in question is related to the effect of *temperature* on the structural relaxation. However, when cooling a liquid isobarically two effects contribute to the slowing down of the dynamics: the decrease of temperature and the associated increase of density. Hence, the isobaric fragility is a combined measure of the two effects. It is of course the underlying goal that the proposed correlations be used as guidelines and tests in the development of theories and models for the glass transition. It is therefore important to clarify whether the correlations result from, and consequently unveil information on, the intrinsic effect of temperature on the relaxation time, the effect of density, or a balanced combination of the two.

Equations (6) and (2) show how isobaric fragility can be decomposed into two contributions, that of temperature being given by m_ρ and the relative effect of density on relaxation time characterized by $\alpha_P T_g \frac{d\log e(\rho)}{d\log \rho}$. Isobaric measurements do not give access to m_ρ or to $\alpha_P T_g \frac{d\log e(\rho)}{d\log \rho}$ independently, but the relevant information can be obtained from data taken under pressure, as we have shown for the data presented here. From this information it becomes possible to revisit the correlations between fragility and other properties [18]. The underlying idea is that a property supposed to correlate to the effect of temperature on the relaxation time should more specifically correlate to the isochoric fragility, m_ρ, than to the isobaric one, m_P.

As also stressed in the introduction, it is instructive to consider the evolution of the empirically established correlations with pressure. As shown in section 2.1, m_ρ is constant, i.e. is independent of density and pressure, when it is evaluated at a pressure- (or density-) dependent T_g corresponding to a given relaxation time. Nonetheless, it follows from equation (6) that the isobaric fragility will in general change due to the pressure dependence of $\alpha_P T_g \frac{d\log e(\rho)}{d\log \rho}$. T_g increases with pressure, $\alpha_P T_g(P)$ decreases, whereas $\frac{d\log e(\rho)}{d\log \rho} = x$ is often to a good approximation constant. As a result, the pressure dependence of m_P is nontrivial. DBP, which we have studied here, shows no significant pressure dependence of the isobaric fragility, while the general behaviour seen from the data compiled by Roland *et al* [13] is that the isobaric fragility decreases or stays constant with pressure, with few exceptions. This seems to indicate that the decrease of $\alpha_P T_g(P)$ usually dominates over the other factors.

The properties that are correlated to fragility will *a priori* also depend on pressure or density. However, if a property is related to the pure effect of temperature on the relaxation time, and therefore correlates to m_ρ, then it should be independent of density when evaluated along an isochrone (usually the glass transition line T_g), as m_ρ itself does not depend on density.

6.2. Stretching and fragility

One of the properties that has been suggested to correlate to the fragility is the nonexponential character of the relaxation function, usually expressed in terms of the stretching parameter β_{KWW}.

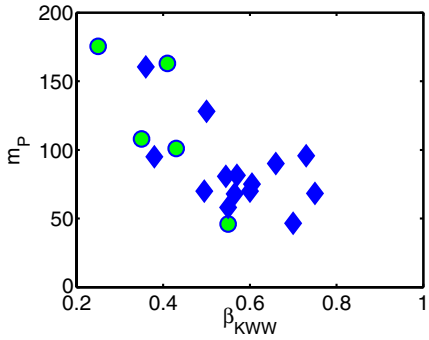

Figure 14. Isobaric fragility as a function of stretching parameter. Diamonds, molecular liquids; circles, polymers. See table 1 for numerical values and references.

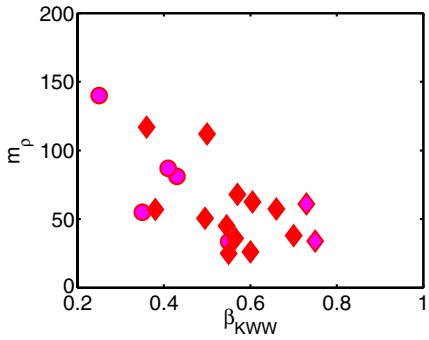

Figure 15. Isochoric fragility m_ρ as a function of stretching parameter. Diamonds, molecular liquids; circles, polymers. See table 1 for numerical values and references.

The data we have reported here confirm the earlier finding [17] that the spectral shape of the alpha relaxation does not vary when pressure is increased while keeping the relaxation time constant. This leads us to suggest that, if a correlation between fragility and stretching does exist, this latter should better correlate to the isochoric fragility which is also independent of pressure than to the isobaric fragility. To test this hypothesis we have collected data from literature reporting isobaric fragility and stretching of the relaxation at T_g. We consider here a description of the shape of the relaxation function in terms of the KWW stretching parameter β_{KWW}. This choice is made because it is convenient to use a characterization with only one parameter for the shape (see appendix B for a discussion and the connection with the Cole–Davidson description used above) and because β_{KWW} is the most reported of the liquids where m_ρ is also available. The compilation of these data is shown in table 1 and in figures 14 and 15, where both the isobaric fragility at atmospheric pressure (figure 14) and isochoric fragility (figure 15) are plotted against the stretching parameter. There is a great deal of scatter in both figures. There is however an observable trend, the fragilities appearing to decrease as the stretching parameter increases. The relative effect of density (over that of temperature) on the slowing down of the relaxation is characterized by the term $\alpha_P T_g \frac{d \log e(\rho)}{d \log \rho} = m_P/m_\rho - 1$. In figure 16 we show the ratio m_P/m_ρ as a function of β_{KWW}. Clearly, no correlation is found between this ratio and the stretching.

The correlation between stretching and fragility is not strikingly different in figures 14 and 15. However, both on theoretical (focusing on the intrinsic effect of temperature) and

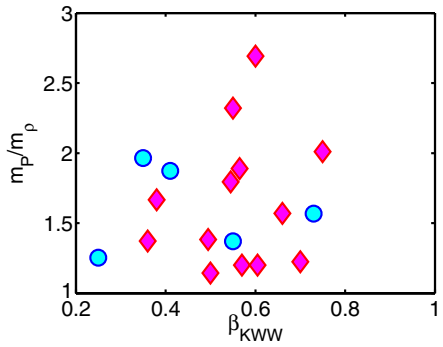

Figure 16. Ratio between isochoric and isobaric fragility as a function of stretching parameter. Diamonds, molecular liquids; circles, polymers. See table 1 for numerical values and references.

Table 1. Fragilities and KWW stretching exponents of molecular liquids and polymers. The * indicates that the value is not given in the corresponding reference but is calculated from the data therein. The following abbreviations are used for the names of the liquids: PC = propylene carbonate, BMPC = 1,1′-bis(*p*-methoxyphenyl)cyclohexane, BMMPC = 1,1′-di(4-methoxy-5-methylphenyl)cyclohexane, KDE = cresolphthalein-dimethyl-ether, DEP A = diglycidylether of bisphenol A, and DHIQ = decahydroisoquinoline.

Compound	m_P	References	m_ρ	References	β_{KWW}	References
o-terphenyl	82, 81, 76, 84	[41–44]	45	[41]	0.57, 0.52	[42, 45]
Dibutyl phthalate	75	This work	63	This work	0.56, 0.65	[29] This work
PC	104, 93, 90	[46, 47, 44]	57, 65*	[48, 15]	0.73	[44]
BMPC	70	[49]	26	[49]	0.6	[50]
BMMPC	58	[48]	25	[48]	0.55	[51]
DEP A	95	[52]	57	[52]	0.38	[53]
KDE	64, 73, 68	[48, 44, 54]	34	[48]	0.75	[44]
DHIQ	163, 158	[55, 47]	117	[55]	0.36	[47]
Cumene	90*	[56]	57*	[56, 57]	0.66	[58]
Salol	68, 73, 63	[13, 44, 59]	36	[13]	0.6, 0.53	[60, 3]
Glycerol	40, 53	[41, 61]	38	[41]	0.65, 0.7, 0.75	[61, 62, 29]
Sorbitol	128	[12]	112	[12]	0.5	[63]
m-fluoroaniline	70	[37]	51*	[15]	0.35, 0.64	[64, 65]
m-toluidine	84, 79	[36, 37]	68	This work	0.57	This work
Polyisobutylene	46	[66]	34*	[39]	0.55	[66]
Polyvinyl chloride	160, 191	[67, 66]	140	[67]	0.25	[66]
Polyvinyl acetate	130, 95, 78	[67, 41, 13]	130, 61, 52	[67, 41, 13]	0.43	[66]
Polystyrene	77, 139	[67, 66]	55	[67]	0.35	[66]
Polymethyl acrylate	102, 122, 102	[67, 52, 66]	80, 94	[67, 52]	0.41	[66]

on phenomenological grounds (isochoric fragility and stretching do not appear to vary as one changes pressure along an isochrone), our contention is that one should prefer using the isochoric fragility.

In the above we have considered only fragility and stretching at the conventional glass transition temperature, that is around $\tau_\alpha = 100$ s. However, we have pointed out in the introduction that both the steepness index characterizing fragility and the stretching parameter depend on the relaxation time. Although still debated, there seems to be a qualitative trend toward a decrease of the stretching (an increase in β_{KWW}) and of the steepness index as the relaxation time decreases and one approaches the 'normal' liquid regime. It would certainly be

very valuable to obtain more data in order to study how the correlation between fragility and stretching evolves as a function of the relaxation time.

7. Conclusion

In this paper we have stressed the constraints that one should put on the search for (meaningful) empirical correlations between the fragility of a glass-former, which characterizes the temperature dependence of the slowing down, and other dynamic or thermodynamic properties. Among such constraints is the check that the proposed correlations, often established at T_g and at atmospheric pressure, are robust when one changes the reference relaxation time (in place of the characteristic of T_g) as well as when one varies the pressure under isochronic conditions. Important also is the fact that fragility depends on the thermodynamic path considered (constant pressure versus constant density) and that, in contrast to the isobaric fragility, the isochoric one appears as an intrinsic property of the glass-former, characterizing the pure effect of temperature.

We have reported dielectric relaxation spectra under pressure for two molecular liquids, *m*-toluidine and DBP. We have combined these data with the available thermodynamic data and analysed the respective effect of density and temperature on the dynamics. Our results are consistent with a general picture in which the isochoric fragility is constant on an isochrone. The shape of the relaxation function, as e.g. expressed by the stretching parameter β_{KWW}, has also been found constant along isochrones.

We have finally discussed the possible correlation between fragility and stretching, suggesting that a meaningful correlation is to be looked for between stretching and isochoric fragility, as both seem to be constant under isochronic conditions and thereby reflect the intrinsic effect of temperature. On the practical side, the correlation is however no stronger with the isochoric fragility than with the isobaric one. One top of large error bars that may be present and that we have addressed in some detail, this reflects the fact that correlations are rather statistical in nature, emerging from a comparison of a large number of glass-formers, rather than one-to-one correspondences between properties of the materials.

Acknowledgments

We would like to thank A Würflinger for the PVT data on *m*-toluidine and Albena Nielsen and co-workers for making available dielectric data on DBP prior to publishing. We are grateful to Denis L'Hôte and François Ladieu for having lent us the SR830 lock-in. Moreover, we acknowledge the work of Joël Jaffré, who built the autoclave for the dielectric measurements under pressure, and Jean-Marie Teuler for help with software. This work was supported by the CNRS (France) and grant No 645-03-0230 from Forskeruddannelsesraadet (Denmark).

Appendix A. Details of the density calculation

The pressure and temperature dependences of the density are of course a crucial input to the scaling shown in section 4.1. In order to evaluate the effect of the extrapolations we have performed, we focus on the scaling for the high-pressure room-temperature data of Paluch on DBP [33] and the data at atmospheric pressure, because the extrapolation of the density is smallest in these cases. The discrepancies seen in figure 5 could be accounted for if the density at high pressure and room temperature were higher than what we have estimated or if the density at low temperature were lower than what we have estimated. The high-density dynamical data are taken at room temperature. The experimental density data are also taken at room temperature and they are only extrapolated above 1.2 GPa. If the actual density is higher

than what we have estimated, then it means that the compressibility is larger than what we have taken. However, the compressibility at 1.2 GPa is already in the high-pressure domain, where it is very low and almost pressure independent (it is slightly decreasing with increasing pressure). The most conservative estimate we could make is to keep the compressibility constant for pressures above the last experimental point at 1.2 GPa. Such an approach changes the ratio $\rho^{2.5}/T$ by less than 1%, and therefore cannot account for the discrepancy seen in figure 5. An alternative explanation would be that the actual low-temperature density is lower than we have estimated, meaning that we have overestimated the expansion coefficient α_P. This latter has been calculated at two different high temperatures based on the data in [30]. This leads to a slight decrease in expansion coefficient with decreasing temperature. If the expansion coefficient is to be smaller than the estimate from this temperature dependence, then it would mean that the temperature dependence of the expansion coefficient should increase as temperature decreases. This is the opposite of what is seen in real liquids, where α_P at atmospheric pressure tends to a constant at low temperatures [32]. It is actually most common to assume that the α_P of molecular liquids is constant below room temperature (e.g. [15]). This type of assumption would enhance the discrepancy in figure 5. We therefore conclude that the absence of collapse of the high-pressure data in figure 5 using a simple power law form for $e(\rho)$ cannot be explained by errors made in the estimating the PVT data.

Appendix B. Characterizing the spectral shape

In the following, we briefly review the procedures commonly used to characterize the shape of the relaxation spectrum of viscous liquids and test different descriptions on one of our spectra. We more specifically look at schemes for converting one type of description to another. This analysis is important for the present work because we compile literature data in section 6.2 in order to look at possible general connections between relaxation shape and temperature dependence of the relaxation time.

The (normalized) Kohlrausch–William–Watts function or stretched exponential, $\phi_{KWW}(t) = \exp[-\left(\frac{t}{\tau}\right)^{\beta_{KWW}}]$, leads to a loss peak in the frequency domain that is given by the one-side Fourier transform

$$\phi''_{KWW}(\omega) = \int_0^\infty -\frac{d\phi_{KWW}(t)}{dt}\sin(\omega t)\,dt. \tag{B.1}$$

The low-frequency behaviour of this function is always a power law with unit exponent. The high-frequency behaviour is a power law with exponent $-\beta_{KWW}$ [68]. β_{KWW} is the only parameter describing the shape of the relaxation function. Hence it controls both the exponent of the high-frequency power law and the width of the relaxation function.

The Havriliak–Negami (HN) function,

$$\phi_{HN}(\omega) = \frac{1}{[1 + (i\omega\tau_{HN})^\alpha]^\gamma}, \tag{B.2}$$

gives a power law with exponent $(-\alpha\gamma)$ in the high-frequency limit and a power law of exponent α in the low-frequency limit of its imaginary part.

The HN function reduces to the Cole–Davidson (CD) one when $\alpha = 1$. (In the case of a CD function we follow the convention and refer to the γ above as β_{CD}.) The CD spectrum has the same general characteristics as the KWW one: a high-frequency power law with exponent given by β_{CD} and a low-frequency power law with exponent one. However, the shape of the two functions is not the same. The CD function is narrower for a given high-frequency exponent (given β) than the KWW function. The best overall correspondence between the CD function and the KWW function has been determined by Lindsey and Patterson [68].

No good correspondence exists in general between the HN and the KWW functions, first of all because the former involves two adjustable shape parameters and the latter only one (plus in both cases a parameter for the intensity and one for the timescale). The KWW function always has a slope of one at low frequencies while the HN function has a generally nontrivial α. Alvarez *et al* [69] numerically found that the two functions can nonetheless be put in correspondence by fixing the relation between the two HN parameters $\gamma = 1 - 0.812(1-\alpha)^{0.387}$ and choosing $\beta_{\mathrm{KWW}} = (\alpha\gamma)^{(1/1.23)}$. This restricted version of the HN function is sometimes referred to as the AAC function [70]. The shape is described by one parameter. However, it is clear that this function cannot correspond to the KWW function in the frequency range where the loss can be described by power laws, as also noted by Gomez and Alegria [70]. The AAC function inherits the behaviour of the HN function; as a result it has a nontrivial exponent α at low frequencies and an exponent $-\alpha\gamma$ at high frequencies, while the associated KWW function has exponents one and $-\beta_{\mathrm{KWW}} = -(\alpha\gamma)^{(1/1.23)}$ at low and high frequencies, respectively.

Another approach is to describe the dielectric spectrum by a distribution of Debye relaxations

$$(\epsilon(\omega) - \epsilon_\infty)/\Delta\epsilon = \int_{-\infty}^{\infty} D(\ln\tau)\frac{1}{1+\mathrm{i}\omega\tau}\mathrm{d}\ln\tau, \tag{B.3}$$

and to fit the shape of the distribution $D(\ln\tau)$ rather than the spectral shape directly. The following form has been suggested for the distribution function [71]:

$$D(\ln\tau) = N\exp\left(-\beta/\alpha(\tau/\tau_0)^\alpha\right)(\tau/\tau_0)^\beta\left(1+\left(\frac{\tau\sigma}{\tau_0}\right)^{\gamma-\beta}\right), \tag{B.4}$$

where N is a normalization factor. The function above is known as the extended generalized gamma distribution, GGE. The last term (and the parameters γ and σ) describes a high-frequency wing, corresponding to a change from one power law behaviour $(-\beta)$ to another $(-\gamma)$. This term can therefore be omitted if no wing is observed in the spectrum. This results in a simpler distribution, the generalized gamma distribution (GG) whose shape is described by two parameters: α determines the width and β gives the exponent of the high-frequency power law. The low frequency is always a power law with exponent one.

Finally, it is possible to describe the spectra phenomenologically in terms of the full width at half maximum, usually normalized to the full width at half maximum of a Debye peak [29] (W/W_{D}, with $W_{\mathrm{D}} = 1.14$ decade), and by the exponent of the power law describing the high-frequency side. The power law exponent is not always well defined, as there can be a high-frequency wing or a secondary process appearing at high frequencies. Olsen *et al* [72] therefore suggest characterizing the alpha peak by the minimal slope found in a double-logarithmic plot of the dielectric loss as a function of frequency. Note that this phenomenological description requires two parameters to describe the shape, while the commonly used CD and the KWW functions use only one parameter to describe the spectrum.

In figure B.1 we show one of the dielectric spectra of *m*-toluidine along with fits to the functions described above. The minimal slope is -0.44 and $W/W_{\mathrm{D}} = 1.56$. The best fits to the different functions are displayed in figure B.1. The CD fit gives $\beta_{\mathrm{CD}} = 0.42$, which with the Lindsey–Patterson scheme [68] corresponds to $\beta_{\mathrm{KWW}} \approx 0.55$. The direct fit with the Fourier transform of the KWW gives $\beta_{\mathrm{KWW}} = 0.57$. The best AAC fit gives $\alpha = 0.85$, leading to $\gamma = 0.61$ and $\beta_{\mathrm{KWW}} \approx (\gamma\alpha)^{1/1.23} = 0.59$. This shows that both the Patterson and the AAC approximations reasonably well reproduce the β_{KWW} value found from using KWW directly. Another point worth noticing is that the β_{KWW} value does not correspond to the actual high-frequency slope of the experimental data in a log–log plot. This is because the overall agreement between the fit and the data is much more governed by the width of the

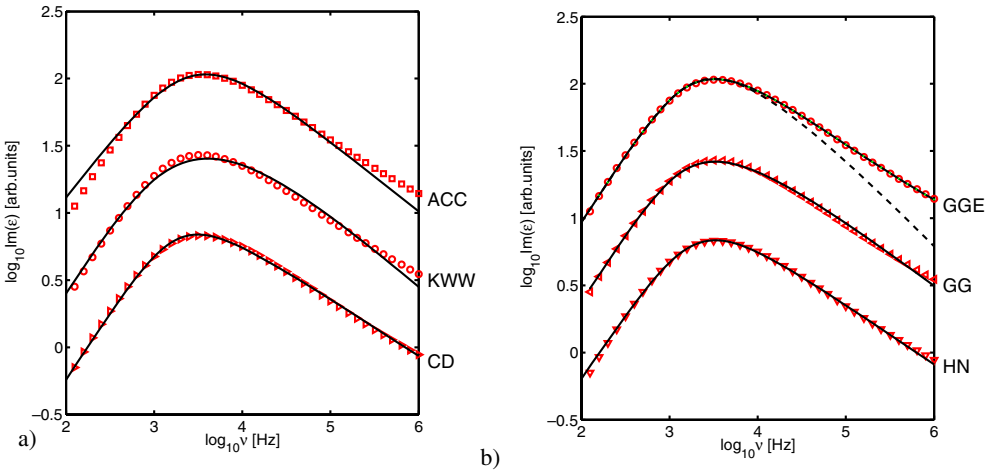

Figure B.1. Log–log plot of the dielectric loss of *m*-toluidine at $T = 216.4$ K and 122 MPa along with best fits to several common functional forms. (a) The fitting functions from the bottom up: CD, KWW, AAC. (b) From the bottom up: HN, gamma distribution, generalized gamma distribution. CD, KWW and AAC have one parameter characterizing the shape, HN and gamma have two and generalized gamma has been fitted using three adjustable parameters. The dashed line shows the gamma distribution corresponding to the generalized gamma distribution. The curves are displaced along the y axis by regular amounts.

relaxation function than by its high-frequency slope, as is also clearly seen for the KWW fit in figure B.1. Note that the AAC approximation for the relation between the HN parameters and β_{KWW} only holds when the HN parameters are fixed according to $\gamma = 1 - 0.812(1-\alpha)^{0.387}$. The original HN function has two adjustable parameters to describe the shape. The best HN fit gives $\alpha = 0.95$ and $\gamma = 0.46$. The gamma distribution which also has two free parameters gives $\alpha = 40$ and $\beta = 0.49$. Finally we have fitted with the GGE using the constraint $\beta = 3\gamma$ (see [73]), meaning that the function has three free parameters to describe the shape, the values being $\alpha = 40$, $\beta = 0.7$, $\sigma = 53$ and $\gamma = \beta/3 = 0.23$. It is not surprising that the GGE with three free parameters gives by far the best fit. However it is also striking that the CD with only one parameter describing the shape gives a good fit over the whole peak, whereas this is not true for the KWW or for the AAC.

From the above we conclude that the CD function gives a good description of the shape of the relaxation using only one parameter to describe the shape. We therefore use this function to fit our data. The KWW exponent, β_{KWW}, does not give a proper measure of the high-frequency slope, but it does give a reasonable one-parameter measure of the overall shape of the dispersion. The KWW function is moreover the function most commonly used in the literature, which is the main reason for using it in the discussion (section 6).

References

[1] Angell C A 1984 Strong and fragile liquids *Relaxations in Complex Systems* ed K L Ngai and G B Wright (Washington, DC: US GPO) p 3

[2] Adam G and Gibbs J H 1965 On temperature dependence of cooperative relaxation properties in glass-forming liquids *J. Chem. Phys.* **43** 139

[3] Böhmer R, Ngai K L, Angell C A and Plazek D J 1993 Nonexponential relaxations in strong and fragile glass formers *J. Chem. Phys.* **99** 4201–9

[4] Sokolov A P, Rössler E, Kisliuk A and Quitmann D 1993 Dynamics of strong and fragile glass formers—differences and correlation with low-temperature properties *Phys. Rev. Lett.* **71** 2062–5
[5] Ngai K L 2000 Dynamic and thermodynamic properties of glass-forming substances *J. Non-Cryst. Solids* **275** 7–51
[6] Scopigno T, Ruocco G, Sette F and Monaco G 2003 Is the fragility of a liquid embedded in the properties of its glass? *Science* **302** 849–52
[7] Novikov V N and Sokolov A P 2004 Poisson's ratio and the fragility of glass-forming liquids *Nature* **431** 961–3
[8] Dyre J C 2006 The glass transition and elastic models of glass-forming liquids *Rev. Mod. Phys.* **78** 953–72
[9] Richert R and Angell C A 1998 Dynamics of glass-forming liquids. V. On the link between molecular dynamics and configurational entropy *J. Chem. Phys.* **108** 9016–26
[10] Alba-Simionesco C, Kivelson D and Tarjus G 2002 Temperature, density, and pressure dependence of relaxation times in supercooled liquids *J. Chem. Phys.* **116** 5033–8
[11] Tarjus G, Kivelson D, Mossa S and Alba-Simionesco C 2004 Disentangling density and temperature effects in the viscous slowing down of glassforming liquids *J. Chem. Phys.* **120** 6135–41
[12] Casalini R and Roland C M 2004 Thermodynamical scaling of the glass transition dynamics *Phys. Rev.* E **69** 062501
[13] Roland C M, Hensel-Bielowka S, Paluch M and Casalini R 2005 Supercooled dynamics of glass-forming liquids and polymers under hydrostatic pressure *Rep. Prog. Phys.* **68** 1405–78
[14] Dreyfus C, Le grand A, Gapinski J, Steffen W and Patkowski A 2004 Scaling the alpha-relaxation time of supercooled fragile organic liquids *Eur. Phys. J.* B **42** 309–19
[15] Reiser A, Kasper G and Hunklinger S 2005 Pressure-induced isothermal glass transition of small organic molecules *Phys. Rev.* B **72** 094204
[16] Floudas G, Mpoukouvalas K and Papadopoulos P 2006 The role of temperature and density on the glass-transition dynamics of glass formers *J. Chem. Phys.* **124** 074905
[17] Ngai K L, Casalini R, Capaccioli S, Paluch M and Roland C M 2005 Do theories of the glass transition, in which the structural relaxation time does not define the dispersion of the structural relaxation, need revision? *J. Phys. Chem.* B **109** 17356–60
[18] Niss K and Alba-Simionesco C 2006 Effects of density and temperature on correlations between fragility and glassy properties *Phys. Rev.* B **74** 024205
[19] Morineau D and Alba-Simionesco C 1998 Hydrogen-bond-induced clustering in the fragile glass-forming liquid *m*-toluidine: experiments and simulations *J. Chem. Phys.* **109** 8494–503
[20] Morineau D, Alba-Simionesco C, Bellissent-funel M C and Lauthie M F 1998 Experimental indication of structural heterogeneities in fragile hydrogen-bonded liquids *Europhys. Lett.* **43** 195–200
[21] Ferrer M L, Lawrence C, Demirjian B G, Kivelson D, Alba-Simionesco C and Tarjus G 1998 Supercooled liquids and the glass transition: temperature as the control variable *J. Chem. Phys.* **109** 8010–5
[22] Alba-Simionesco C and Tarjus G 2006 Temperature versus density effects in glassforming liquids and polymers: a scaling hypothesis and its consequences *J. Non-Cryst. Solids* **352** 4888–94
[23] Schug K U, King H E and Böhmer R 1998 Fragility under pressure: diamond anvil cell viscometry of ortho-terphenyl and salol *J. Chem. Phys.* **109** 1472
[24] Granato A V 2002 The specific heat of simple liquids *J. Non-Cryst. Solids* **307** 376–86
[25] Dyre J C and Olsen N B 2004 Landscape equivalent of the shoving model *Phys. Rev.* E **69** 042501
[26] Kivelson D and Tarjus G 1998 SuperArrhenius character of supercooled glass-forming liquids *J. Non-Cryst. Solids* **235** 86
[27] Sekula M, Pawlus S, Hensel-bielowka S, Ziolo J, Paluch M and Roland C M 2004 Structural and secondary relaxations in supercooled di-n-butyl phthalate and diisobutyl phthalate at elevated pressure *J. Phys. Chem.* B **108** 4997–5003
[28] Fujimori H, Oguni M and Alba-Simionesco C 1997 Pressure effect as referred to the temperature effect on irreversible structural relaxations in liquid dibutylphthalate *Prog. Theor. Phys. Suppl.* **126** 235–8
[29] Dixon P K, Wu L, Nagel S R, Williams B D and Carini J P 1990 Scaling in the relaxation of supercooled liquids *Phys. Rev. Lett.* **65** 1108–11
[30] Bridgman P W 1932 Volume–temperature–pressure relations for several non-volatile liquids *Proc. Am. Acad. Arts Sci.* **67** 1–27
[31] Cook R L, Herbst C A and King H E 1993 High-pressure viscosity of glass-forming liquids measured by the centrifugal force diamond anvil cell viscometer *J. Phys. Chem.* **97** 2355–61
[32] Terminassian L, Bouzar K and Alba C 1988 Thermodynamic properties of liquid toluene *J. Phys. Chem.* **92** 487–93
[33] Paluch M, Sekula M, Pawlus S, Rzoska S J, Ziolo J and Roland C M 2003 Test of the Einstein–Debye relation in supercooled dibutylphthalate at pressures up to 1.4 GPa *Phys. Rev. Lett.* **90** 175702

[34] Roland C M, Bair S and Casalini R 2006 Thermodynamic scaling of the viscosity of van der Waals, H-bonded, and ionic liquids *J. Chem. Phys.* **125** 124508
[35] Nielsen A, Cristensen T, Olsen N B and Dyre J C 2006 unpublished data
[36] Mandanici A, Cutroni M and Richert R 2005 Dynamics of glassy and liquid *m*-toluidine investigated by high-resolution dielectric spectroscopy *J. Chem. Phys.* **122** 084508
[37] Alba-Simionesco C, Fan J and Angell C A 1999 Thermodynamic aspects of the glass transition phenomenon. II. Molecular liquids with variable interactions *J. Chem. Phys.* **110** 5262–72
[38] Alba-Simionesco C, Fujimori H, Morineau D and Frick B 1997 A study of the glass transition of molecular liquids as a function of pressure and temperature *Prog. Theor. Phys. Suppl.* **126** 229–33
[39] Chauty-Cailliaux A 2003 Thermodynamique, structure, et dynamique de polymeres amporphes sous pression a l'appoche de la transition vitreuse *PhD Thesis* Universite Paris XI
[40] Würflinger A, private communication data
[41] Alba-Simionesco C, Cailliaux A, Alegria A and Tarjus G 2004 Scaling out the density dependence of the a relaxation in glass-forming polymers *Europhys. Lett.* **68** 58–64
[42] Dixon P K and Nagel S R 1988 Frequency-dependent specific-heat and thermal-conductivity at the glass-transition in ortho-terphenyl mixtures *Phys. Rev. Lett.* **61** 341–4
[43] Huang D H and Mckenna G B 2001 New insights into the fragility dilemma in liquids *J. Chem. Phys.* **114** 5621–30
[44] Paluch M, Ngai K L and Hensel-bielowka S 2001 Pressure and temperature dependences of the relaxation dynamics of cresolphthalein-dimethylether: evidence of contributions from thermodynamics and molecular interactions *J. Chem. Phys.* **114** 10872–83
[45] Tölle A 2001 Neutron scattering studies of the model glass former ortho-terphenyl *Rep. Prog. Phys.* **64** 1473–532
[46] Qin Q and McKenna G B 2006 Correlation between dynamic fragility and glass transition temperature for different classes of glass forming liquids *J. Non-Cryst. Solids* **352** 2977–85
[47] Richert R, Duvvuri K and Duong L T 2003 Dynamics of glass-forming liquids. VII. Dielectric relaxation of supercooled *tris*-naphthylbenzene, squalane, and decahydroisoquinoline *J. Chem. Phys.* **118** 1828
[48] Casalini R and Roland C M 2005 Scaling of the supercooled dynamics and its relation to the pressure dependences of the dynamic crossover and the fragility of glass formers *Phys. Rev.* B **71** 014210
[49] Casalini R and Roland C M 2005 Temperature and density effects on the local segmental and global chain dynamics of poly(oxybutylene) *Macromolecules* **38** 1779–88
[50] Hensel-bielowka S, Ziolo J, Paluch M and Roland C M 2002 The effect of pressure on the structural and secondary relaxations in 1,1′-bis (*p*-methoxyphenyl) cyclohexane *J. Chem. Phys.* **117** 2317–23
[51] Casalini R, Paluch M and Roland C M 2003 Influence of molecular structure on the dynamics of supercooled van der Waals liquids *Phys. Rev.* E **67** 031505
[52] Roland C M, Paluch M, Pakula T and Casalini R 2004 Volume and temperature as control parameters for the dielectric a relaxation of polymers and molecular glass formers *Phil. Mag.* **84** 1573–81
[53] Paluch M, Roland C M, Gapinski J and Patkowski A 2003 Pressure and temperature dependence of structural relaxation in diglycidylether of bisphenol a *J. Chem. Phys.* **118** 3177–86
[54] Roland C M and Casalini R 2003 Temperature dependence of local segmental motion in polystyrene and its variation with molecular weight *J. Chem. Phys.* **119** 1838–42
[55] Casalini R, McGrath K J and Roland C M 2006 Isobaric and isochoric properties of decahydroisoquinoline an extremly fragile glass former *J. Non-Cryst. Solids* **352** 4905–9
[56] Barlow A J, Lamb J and Matheson A J 1966 Viscous behaviour of supercooled liquids *Proc. R. Soc.* A **292** 322
[57] Bridgman P W 1949 Viscosities to 30 000 kg/cm^2 *Proc. Am. Chem. Soc.* **77** 129
[58] Niss K, Dalle-Ferrier C and Alba-Simionesco C 2006 unpublished data
[59] Laughlin W T and Uhlmann D R 1972 Viscous flow in simple organic liquids *J. Phys. Chem.* **76** 2317
[60] Sidebottom D L and Sorensen C M 1989 Light-scattering study of the glass-transition in salol *Phys. Rev.* B **40** 461–6
[61] Birge N O 1986 Specific-heat spectroscopy of glycerol and propylene-glycol near the glass-transition *Phys. Rev.* B **34** 1631–42
[62] Ngai K L and Rendell R W 1990 Comparison between frequency-dependent specific-heat and dielectric-relaxation of glycerol and propylene-glycol *Phys. Rev.* B **41** 754–6
[63] Ngai K L, Rendell R W and Plazek D J 1991 Couplings between the cooperatively rearranging regions of the Adam–Gibbs theory of relaxations in glass-forming liquids *J. Chem. Phys.* **94** 3018–29
[64] Cutroni M, Migliardo P, Piccolo P A and Alba-Simionesco C 1994 The dynamic glass-transition of a fragile molecular liquid in the megahertz domain *J. Phys.: Condens. Matter* **6** 5283–93
[65] Hensel-bielowka S, Paluch M and Ngai K L 2005 Emergence of the genuine Johari–Goldstein secondary relaxation in m-fluoroaniline after suppression of hydrogen-bond-induced clusters by elevating temperature and pressure *J. Chem. Phys.* **123** 014502

[66] Plazek D J and Ngai K L 1991 Correlation of polymer segmental chain dynamics with temperature-dependent time-scale shifts *Macromolecules* **24** 1222–4
[67] Huang D H, Colucci D M and Mckenna G B 2002 Dynamic fragility in polymers: a comparison in isobaric and isochoric conditions (vol 116, pg 3925, 2002) *J. Chem. Phys.* **117** 7390
[68] Lindsey C P and Patterson G D 1980 Detailed comparison of the Williams–Watts and Cole–Davidson functions *J. Chem. Phys.* **73** 3348–57
[69] Alvarez F, Alegria A and Colmenero J 1991 Relationship between the time-domain Kohlrausch–Williams–Watts and frequency-domain Havriliak–Negami relaxation functions *Phys. Rev.* B **44** 7306–12
[70] Gomez D and Alegria A 2001 On the empirical functions describing the alpha-relaxation of glass-forming systems *J. Non-Cryst. Solids* **287** 246–51
[71] Blochowicz T, Tschirwitz C, Benkhof S and Rössler E A 2003 Susceptibility functions for slow relaxation processes in supercooled liquids and the search for universal relaxation patterns *J. Chem. Phys.* **118** 7544–55
[72] Olsen N B, Christensen T and Dyre J C 2001 Time-temperature superposition in viscous liquids *Phys. Rev. Lett.* **86** 1271
[73] Blochowicz T, Gainaru C, Medick P, Tschirwitz C and Rossler E A 2006 The dynamic susceptibility in glass forming molecular liquids: the search for universal relaxation patterns II *J. Chem. Phys.* **124** 134503